Molecular Biology of the Cell
Vol. 19, 414–423, January 2008

Ca^{2+}-dependent Calmodulin Binding to FcRn Affects Immunoglobulin G Transport in the Transcytotic Pathway

Bonny L. Dickinson,[*†] Steven M. Claypool,[‡] June A. D'Angelo,[*†] Martha L. Aiken,[*†] Nanda Venu,[§] Elizabeth H. Yen,[§] Jessica S. Wagner,[§‖] Jason A. Borawski,[§] Amy T. Pierce,[*†] Robert Hershberg,[¶] Richard S. Blumberg,[‡‖] and Wayne I. Lencer[§‖]

[*]The Research Institute for Children, Children's Hospital, Department of Pediatrics, New Orleans, LA 70118; [†]Department of Microbiology, Immunology, and Parasitology, Louisiana State University Health Science Center, New Orleans, LA 70112; [‡]Division of Gastroenterology, Brigham and Women's Hospital and the Department of Medicine, Harvard Medical School, Boston, MA 02115; [§]Gastrointestinal Cell Biology, Division of Pediatric Gastroenterology and Nutrition, Children's Hospital and the Department of Pediatrics, Harvard Medical School, Boston, MA 02115; [¶]Department of Medicine and Medical Genetics, University of Washington School of Medicine, Seattle, WA 98112; and [‖]Harvard Digestive Diseases Center, Boston, MA 02115

Submitted July 11, 2007; Revised October 9, 2007; Accepted November 2, 2007
Monitoring Editor: Keith Mostov

The Fcγ receptor FcRn transports immunoglobulin G (IgG) so as to avoid lysosomal degradation and to carry it bidirectionally across epithelial barriers to affect mucosal immunity. Here, we identify a calmodulin-binding site within the FcRn cytoplasmic tail that affects FcRn trafficking. Calmodulin binding to the FcRn tail is direct, calcium-dependent, reversible, and specific to residues comprising a putative short amphipathic α-helix immediately adjacent to the membrane. FcRn mutants with single residue substitutions in this motif, or FcRn mutants lacking the cytoplasmic tail completely, exhibit a shorter half-life and attenuated transcytosis. Chemical inhibitors of calmodulin phenocopy the mutant FcRn defect in transcytosis. These results suggest a novel mechanism for regulation of IgG transport by calmodulin-dependent sorting of FcRn and its cargo away from a degradative pathway and into a bidirectional transcytotic route.

INTRODUCTION

The major histocompatibility complex (MHC) class I-related receptor FcRn functions to traffic immunoglobulin G (IgG) across polarized epithelial cells that line mucosal surfaces (Dickinson *et al*., 1999; Claypool *et al*., 2002, 2004; Spiekermann *et al*., 2002). Unlike the polymeric immunoglobulin receptor that mediates the polarized secretion of dimeric IgA and pentameric IgM, FcRn moves IgG in both directions across epithelial barriers so as to provide a dynamic exchange between circulating and lumenal IgG at mucosal sites. Uniquely, FcRn is one of the few proteins to move inward from the apical-to-basolateral membrane, a pathway poorly understood but highly significant for the absorption of environmental antigens and microbial products. Recent studies in mice transgenic for human FcRn show that such trafficking by FcRn provides a way for IgG to participate in immune surveillance and host defense (Bitonti *et al*., 2004; Yoshida *et al*., 2004, 2006). FcRn has another trafficking function especially prominent in vascular endothelial cells. In this tissue, FcRn binds IgG internalized by fluid phase endocytosis and recycles the immunoglobulin back into the circulation, thereby salvaging IgG from lysosomal degradation and increasing its half-life (Borvak *et al*., 1998; Ward *et al*., 2003).

The molecular mechanisms that dictate how FcRn traffics IgG in the recycling and transcytotic pathways remain to be elucidated. Both transport pathways are likely regulated by multiple and hierarchically ordered sorting determinants within the receptor. Studies on human and rat FcRn show that basolateral targeting results from motifs present within the cytoplasmic tail (Stefaner *et al*., 1999; McCarthy *et al*., 2001; Wu and Simister, 2001; Claypool *et al*., 2004). The signals that orchestrate FcRn transport to the apical membrane domain, and back again to the basolateral membrane, or away from the lysosome, are unknown.

Structurally, the extracellular domain of FcRn folds almost exactly like the MHC class I (MHC I) molecule, requiring stable assembly with light chain β2-microglobulin (β_2m) for function; but the peptide binding groove apparent in the MHC I heavy chain is closed in FcRn (Huber *et al*., 1993; Burmeister *et al*., 1994). Another region of this domain functions to bind IgG. Unlike other Fcγ receptors, FcRn binds IgG only at acidic pH (pH ≤ 6.5) and releases it at neutral pH (pH ≥ 7.4) (Rodewald, 1976; Raghavan *et al*., 1993). The

This article was published online ahead of print in *MBC in Press* (http://www.molbiolcell.org/cgi/doi/10.1091/mbc.E07–07–0658) on November 14, 2007.

Address correspondence to: Wayne I. Lencer (wayne.lencer@childrens.harvard.edu).

Abbreviations used: β2m, β-2-microglobulin; CaM, calmodulin; CaM-Seph, calmodulin-Sepharose; GST, glutathione transferase; HA, influenza hemagglutinin epitope; Ig, immunoglobulin; mAb, monoclonal antibody; MDCK, Madin-Darby canine kidney; NIP, 5-iodo-4-hydroxy-3-nitrophenylacetyl.

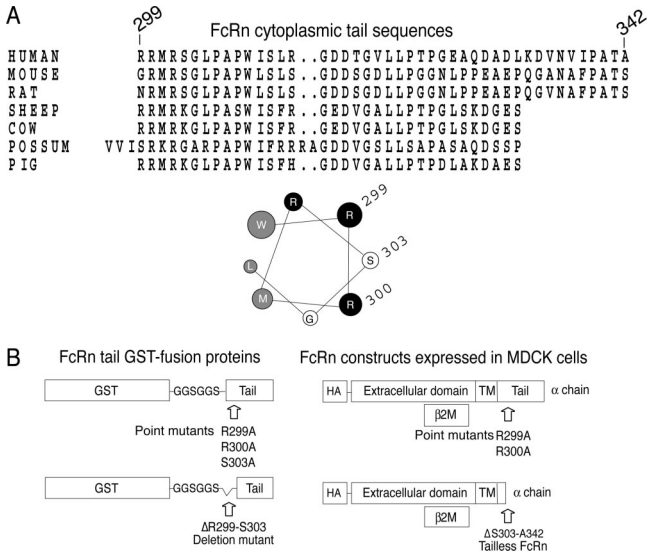

Figure 1. The FcRn cytoplasmic tail contains a putative calmodulin-binding motif. (A) Sequence alignment of the human, mouse, rat, sheep, cow, possum, and pig FcRn cytoplasmic tails. Sequences are displayed from the FcRn N terminus and numbered according to their appearance in the human FcRn tail sequence. A helical wheel projection of the membrane-proximal residues of the human FcRn cytoplasmic tail reveals a putative amphipathic α-helix. One face of the helix is composed of basic, positively charged residues (black) and the opposite face contains hydrophobic residues (gray). (B) Schematic of FcRn tail GST-fusion proteins used for in vitro pull-down assays (left) and HA-tagged human FcRn constructs expressed in MDCK cells (right). TM, transmembrane domain.

amino acid sequence of the FcRn cytoplasmic domain differs significantly from that of MHC I. In FcRn, the cytoplasmic tail contains both dileucine and tryptophan endocytosis motifs and several serine phosphorylation sites that affect the polarity of cell surface expression and intracellular trafficking (Stefaner *et al*., 1999; McCarthy *et al*., 2001; Wu and Simister, 2001; Zhao *et al*., 2003). To date, no structure–function studies in the FcRn transmembrane domain have been performed.

In this study, we examine the idea that FcRn trafficking may be regulated by calmodulin. Our interest in calmodulin arose from the observation that the membrane-proximal region of the FcRn tail is highly conserved among mammalian species and that it contains an amino acid sequence with the potential to form a short amphipathic α-helix (Figure 1A). Amphipathic α-helices can function as calmodulin-binding motifs (Rhoads and Friedberg, 1997; Chin and Means, 2000), and they are recently recognized as domains capable of sensing or perturbing membrane curvature so as to affect protein sorting (McMahon and Gallop, 2005). Thus, binding to calmodulin may be one way that trafficking of FcRn is physiologically regulated. Here, we show that calmodulin binds directly to the FcRn cytoplasmic tail domain, and that FcRn mutants unable to bind calmodulin exhibit a shorter half-life and attenuated transcytosis across polarized epithelial cells. These results suggest a novel mechanism for sorting FcRn and its cargo between degradative and transcytotic pathways with likely consequences for antigen transport across mucosal surfaces, mucosal immunity, and host defense.

MATERIALS AND METHODS

Plasmids and Recombinant Proteins

The human FcRn cytoplasmic tail was polymerase chain reaction (PCR) amplified and subcloned into pGEX 4-T-3 (GE Healthcare, Piscataway, NJ). The forward primer contained a six amino-acid spacer (GGSGGS) to separate glutathione transferase (GST) from the FcRn tail sequences. GST and FcRn tail GST-fusion proteins were affinity purified on glutathione agarose from BL21 DE3 *Escherichia coli* as per the manufacturer's instructions. Mutations were introduced into the FcRn cytoplasmic tail by overlapping PCR extension mutagenesis and constructs were verified by DNA sequencing as described previously (Claypool *et al*., 2002, 2004). The FcRn heavy chain cDNA was subcloned into a retroviral construct and expressed under the control of the cytomegalovirus IE promoter. Retroviral transduction and generation of stable transfectants was performed as described previously (Hershberg *et al*., 1997; Colgan *et al*., 1999).

Antibodies

Human IgG was purchased from Lampire Biological Laboratories (Pipersville, PA), and chicken IgY was from Gallus Immunotech (Wildwood, MO). Mouse anti-GP135 monoclonal antibody (mAb) was a kind gift from Karl Matlin (Harvard Medical School, Boston, MA) originally obtained from George Ojakian (Department of Anatomy and Cell Biology, SUNY-Downstate Medical Center, Brooklyn, NY). Rabbit polyclonal antisera raised against a GST-human FcRn cytoplasmic tail fusion protein and mAb 12CA5, reactive against the hemagglutinin (HA) epitope, have been described previously (Claypool *et al*., 2002). High-affinity rat anti-HA mAb was purchased from Roche Molecular Biochemicals (Mannheim, Germany). Mouse monoclonal antibodies against β-actin and zona occludens-1, and horseradish peroxidase- and alkaline phosphatase-conjugated secondary antibodies were purchased from Sigma-Aldrich (St. Louis, MO). Two calmodulin antibodies were used, a mouse monoclonal was purchased from Upstate Biotechnology (Chicago, IL) and a rabbit polyclonal antiserum was purchased from Calbiochem (La Jolla, CA). Alexa-conjugated secondary antibodies and phalloidin-Texas Red were from Invitrogen (Carlsbad, CA).

Cell Lines

Madin Darby canine kidney (MDCK) strain II cells expressing wild type (WT) and mutant human FcRn heavy and light chains were cultured as described previously (Claypool *et al*., 2002, 2004). The human intestinal epithelial cell line T84 was a kind gift from Kim Barrett (University of California, San Diego, CA), and it was cultured as described previously (Dickinson *et al*., 1999). Mouse myeloma cell line J558L secreting a 5-iodo-4-hydroxy-3-nitrophenacetyl (NIP)-specific mAb containing the human IgG1 Fc domain (Nip-IgG) was cultured and the antibody affinity purified as described previously (Claypool *et al*., 2004).

Calmodulin-Sepharose Pull-Down Experiments

Soluble GST or FcRn tail GST-fusion proteins were incubated with calmodulin-Sepharose or unconjugated Sepharose beads in intracellular lysis buffer (150 mM potassium acetate, 5 mM sodium acetate, 2.5 mM magnesium chloride, 2 μg of bovine serum albumin, 0.5% NP-40, and 25 mM HEPES, pH 7.3) containing 2 mM $CaCl_2$ or 10 mM EGTA. Fusion proteins associated with the beads were detected by immunoblot with a rabbit anti-GST-human FcRn cytoplasmic tail antiserum. To test whether binding is reversible, fusion proteins were first bound to calmodulin-Sepharose in the presence of $CaCl_2$ and then washed with lysis buffer containing EGTA. In other experiments, GST-tail fusion proteins were tested for binding to calmodulin-Sepharose in intracellular buffer containing Triton X-100 in lieu of NP-40.

FcRn-Calmodulin Coimmunoprecipitation

T84 cell lysates were equilibrated in intracellular lysis buffer containing 2 mM $CaCl_2$ or 10 mM EGTA and incubated with protein G-Sepharose beads chemically conjugated to a mouse anti-calmodulin mAb, or with a mouse anti-calmodulin mAb and protein G-Sepharose beads. MDCK cells expressing human FcRn were lysed in intracellular lysis buffer as described above and incubated with rabbit anti-calmodulin polyclonal antibodies and protein G-Sepharose beads, or with calmodulin-Sepharose (CaM-Seph) beads. FcRn associated with the beads was detected by immunoblot.

IgG-Sepharose Pull-Down Experiments

IgG-Sepharose affinity isolation of FcRn was performed as described previously (Claypool *et al*., 2002).

Selective Cell Surface Biotinylation

Selective cell surface biotinylation was performed as described previously (Claypool *et al*., 2004). Total cellular FcRn present in 5 μg of whole cell lysate (representing 1% of the lysate incubated with avidin-agarose beads) and biotinylated FcRn (representing 75% of the sample eluted from the avidin-agarose beads) were detected by immunoblot. Blots were stripped and re-

probed for GP135. The mass of FcRn on the apical or basolateral membrane was determined by densitometry and expressed as a percentage of total cellular FcRn.

Endocytosis

Endocytosis was performed as described previously (Claypool *et al*., 2002, 2004). Briefly, cells were biotinylated on their basolateral aspect with sulfosuccinimidyl 2-(biotinamido)-ethyl-1,3-dithiopropionate (sulfo-NHS-SS-biotin) at 4°C and either maintained at 4°C for the duration of the experiment or incubated at 37°C for 1, 2, 4, or 8 min and then rapidly cooled to 4°C. Two Transwells per clone were maintained at 4°C as a control (no reduction, time 0) and as a control for reduction (M, mock). Cell surface-associated biotin was stripped by incubation with reduced glutathione at 4°C. After extensive washing to remove glutathione, cells were lysed in radioimmunoprecipitation assay (RIPA) buffer (1 M NaCl, 1 M Tris, pH 8, 10% NP-40, 10% SDS, and 5% sodium deoxycholate) and clarified by centrifugation. Equal quantities of cell lysates (assessed by protein content) were added to avidin-agarose beads and biotinylated FcRn was affinity isolated and measured by SDS-polyacrylamide gel electrophoresis (PAGE) and immunoblot by using the mAb against the HA tag (12CA5). The mass of biotinylated FcRn was determined by densitometry and expressed as a percentage of biotinylated FcRn at time 0.

Transcytosis

Transcytosis of biotinylated human IgG across T84 cell monolayers was performed as described previously (Dickinson *et al*., 1999) with the modification that cells were pretreated with vehicle alone (dimethyl sulfoxide; DMSO) or 30 μM *N*-(6-aminohexyl)-5-chloro-1-naphthalenesulfonamide (W-7) (Calbiochem) in DMSO for 30 min. Transport of biotinylated IgG was analyzed by avidin-horseradish peroxidase (HRP) immunoblot to detect IgG heavy and light chains. Transcytosis of Nip-IgG across MDCK cell monolayers was performed as described previously (Claypool *et al*., 2004). Briefly, cells were pretreated with buffer or buffer containing 30 or 50 μM *N*-(6-aminohexyl)-1-naphthalenesulfonamide (W-5) or W-7 (Calbiochem) (both dissolved in water) for 30 min before the addition of 60 nM Nip-IgG to the apical or basolateral chamber and incubation at 37°C for 120 min. Transcytosis of NIP-IgG into the contralateral chamber was measured using a NIP-specific enzyme-linked immunosorbent assay (ELISA), and the means ± SEM are plotted. Data are normalized to Nip-IgG transport for untreated control MDCK cells expressing WT FcRn clone 13 (=100%). In each experiment, MDCK cell clones were plated and analyzed in triplicate.

Half-Life of Cell Surface-associated FcRn

MDCK cells expressing FcRn were cultured on 1-cm^2 Transwell filters. The basolateral membranes were biotinylated at 4°C and transferred to medium and incubated at 37°C for 0, 6, 12, and 24 h, or for 0, 3, 6, 9, and 12 h. At each time point, cells were lysed in RIPA buffer, and equal quantities of cell lysates (assessed by protein content) were incubated with avidin-agarose beads. FcRn associated with the beads was detected by immunoblot with 12CA5.

Metabolic Labeling

MDCK cells expressing FcRn were cultured on 5-cm^2 Transwell inserts. Cells were preincubated in L-methionine- and L-cysteine-free medium (Sigma-Aldrich) and then labeled with [^{35}S]methionine/cysteine (~280 μm/Transwell; EasyTag Express Protein Labeling Mix, PerkinElmer Life and Analytical Sciences, Boston, MA) for 30 min. After labeling, cells were transferred to medium and incubated at 37°C for 0, 6, 12, 24, and 48 h. At each time point, cells were lysed in RIPA buffer, and FcRn was immunoprecipitated from equal quantities of cell lysates (assessed by protein content) with a rat anti-HA mAb and protein G-Sepharose beads. Proteins associated with the beads were separated by SDS-PAGE, and dried gels were exposed to film (Kodak MR; Eastman Kodak, Rochester, NY). Data are normalized to the average mass of ^{35}S-FcRn present at the 6-h interval (45 ± 4.3%) relative to time 0 h (100%).

Immunocytochemistry and Confocal Microscopy

Immunocytochemical detection of FcRn and ZO-1 in MDCK cells expressing FcRn was performed as described previously (Claypool *et al*., 2004). Briefly, cells were viewed with a Nikon Eclipse E800 microscope equipped with an MRC-1024 confocal system (Bio-Rad, Hercules, CA). Images were collected with a 20× objective (Plan Apo air, numerical aperture 0.75 dual-frequency interferometric confocal microscope, wd 1.0, infinity/0.17) by using Lasersharp (Bio-Rad) acquisition software. Cells were stained with Alexa-conjugated secondary antibodies or phalloidin-Texas Red and fixed for viewing with ProLong anti-fade mounting medium (Invitrogen). Images were processed with Adobe Photoshop and Adobe Illustrator (Adobe Systems, San Jose, CA).

Statistics

Data were analyzed for statistical significance by single-factor analysis of variance (Microsoft, Redmond, WA).

RESULTS

Calmodulin Binds the FcRn Cytoplasmic Tail

To test whether calmodulin binds to the membrane-proximal region of the FcRn cytoplasmic tail, we prepared GST fusion proteins containing the WT FcRn tail domain separated from the GST moiety by a short hydrophilic linker (GGSGGS). We also prepared four similar fusion proteins containing mutations in the membrane-proximal sequence (Figure 1B, left). Two of the mutant fusion proteins contain single amino-acid substitutions that replace alanine for arginine at positions 299 (R299A) and 300 (R300A). A third mutant contains a deletion in which the first five residues of the tail are removed (ΔR299-S303; Del). These mutations will disrupt the charge distribution in the α-helix or delete it entirely. A fourth fusion protein was constructed as a negative control to contain a single amino acid substitution replacing alanine for serine at position 303 (S303A). This substitution is predicted to have no effect on the amphipathic nature of the helix.

In initial studies, the WT FcRn-tail GST-fusion protein or GST alone were incubated with CaM-Seph in the presence or absence of calcium (Ca^{2+}) and tested for binding by SDS-PAGE and immunoblot by using a rabbit polyclonal antiserum raised against a GST-human FcRn cytoplasmic tail fusion protein. This antiserum also detects full-length FcRn

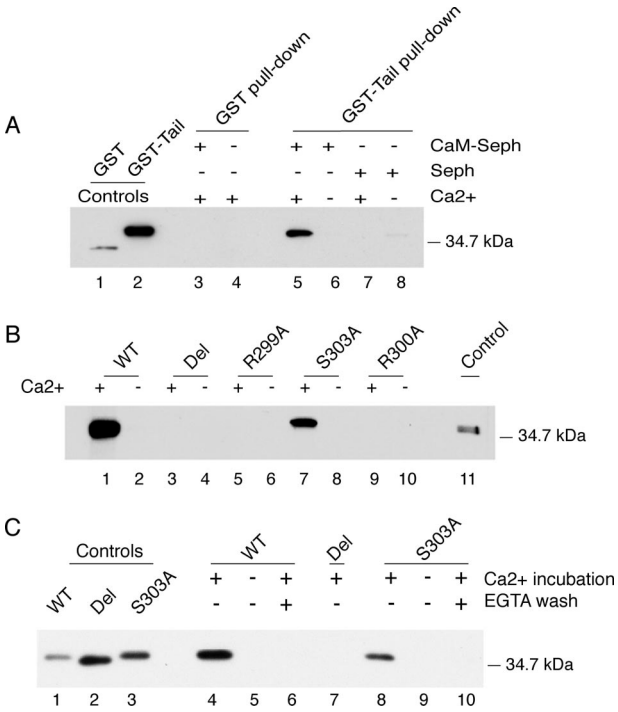

Figure 2. Calmodulin binding to the FcRn cytoplasmic tail is specific, calcium-dependent, and reversible. (A) GST and the WT FcRn tail expressed as a GST fusion protein were incubated with CaM-Seph or Seph. GST and GST-tail proteins are shown as controls in lanes 1 and 2, respectively. Results are representative of four independent experiments. (B) WT and mutant GST-tail fusion proteins were incubated with CaM-Seph in the presence or absence of calcium. WT GST-tail protein is a control in lane 11. Results are representative of four independent experiments. (C) WT and mutant GST-tail fusion proteins were incubated with CaM-Seph in the presence or absence of calcium, and beads were washed with buffers containing calcium or EGTA. Fusion proteins are shown as controls in lanes 1–3. In each experiment, GST-fusion protein binding was assessed by immunoblot. Del, deletion mutant.

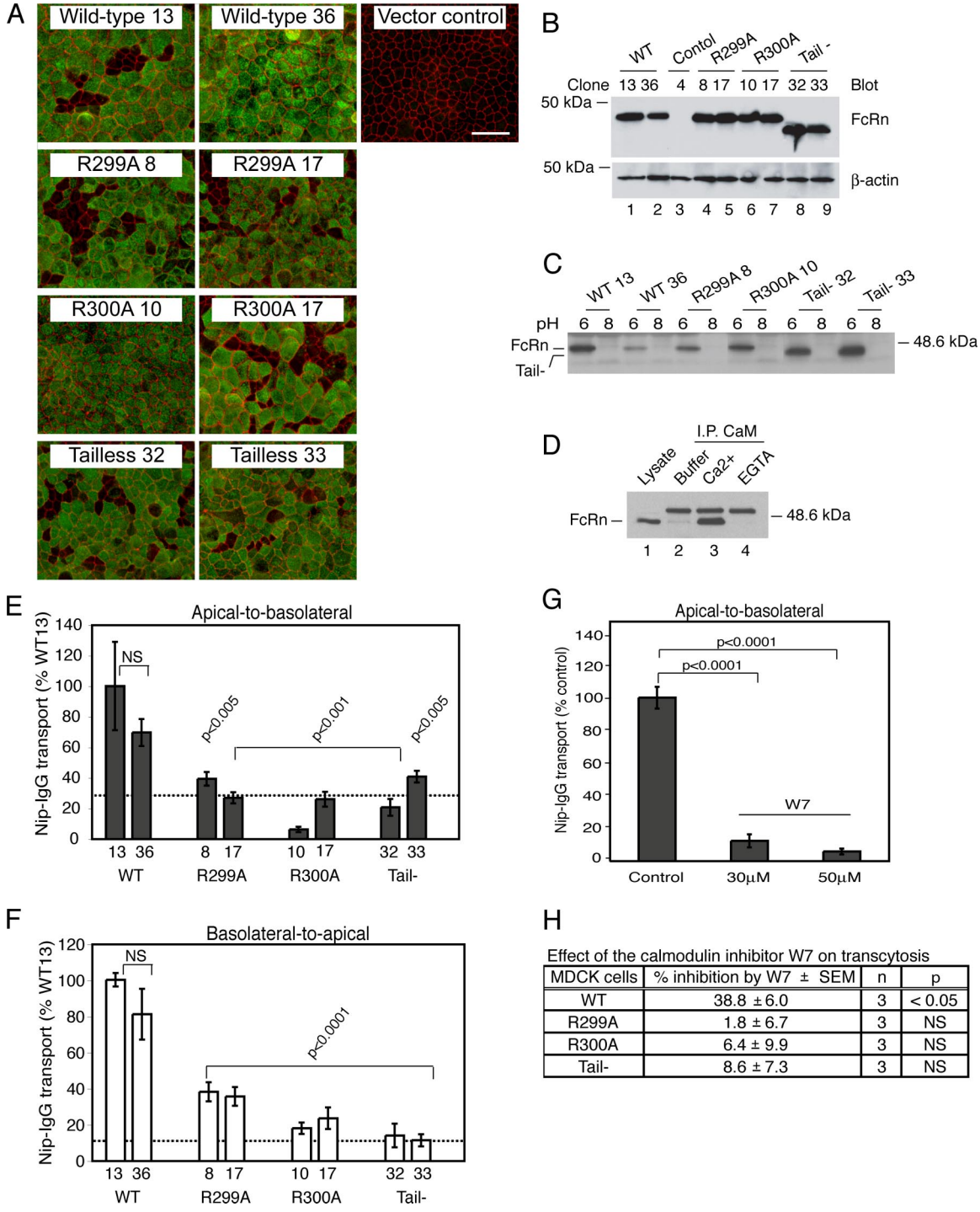

MDCK cells	% inhibition by W7 ± SEM	n	p
WT	38.8 ± 6.0	3	< 0.05
R299A	1.8 ± 6.7	3	NS
R300A	6.4 ± 9.9	3	NS
Tail-	8.6 ± 7.3	3	NS

Figure 3. Calmodulin regulates FcRn-dependent bidirectional IgG transcytosis in MDCK cells. (A) En face confocal images of polarized MDCK cells cultured on Transwell filters. FcRn was detected with an anti-HA mouse mAb (green) and ZO-1 with a rabbit anti-ZO-1 polyclonal antibody (red). Bar, 100 μm. A control clone carrying empty expression plasmid is included (vector control). (B) FcRn expression was assessed in MDCK cells expressing WT FcRn (lanes 1 and 2) and FcRn mutants (lanes 4–9) by immunoblot of whole cell lysates (top). Blots were stripped and reprobed for β-actin to demonstrate equal loading (bottom). Two independently derived clones per construct were analyzed, and a MDCK clone carrying empty expression plasmids is included as a negative control (lane 3). (C) MDCK cells expressing WT or mutant FcRn were lysed in 3-[(3-cholamidopropyl)dimethylammonio]propanesulfonate buffer, pH 6 or 8, and incubated with IgG-Sepharose beads. FcRn binding was examined by immunoblot. Results are representative of four independent experiments. (D) FcRn-calmodulin coimmunoprecipitation was assessed by preparing lysates of MDCK cells expressing WT FcRn in lysis buffer alone (lane 2) or lysis buffer containing calcium (lane 3) or EGTA (lane 4). Lysates were incubated with rabbit anti-calmodulin polyclonal antibodies and protein G-Sepharose beads. FcRn associated with the beads was detected by immunoblot. The top band detected in lanes containing protein G-Sepharose beads (lanes 2–4) is a contaminant released from the beads during sample preparation. The bottom band represents the FcRn heavy chain (~45 kDa) as shown in the whole cell lysate control (lane 1). (E and F) MDCK cell clones expressing WT or mutant FcRn were cultured on Transwell inserts and examined for apical-to-basolateral (E) and basolateral-to-apical (F) transcytosis of Nip-IgG. Two indepen-

expressed in T84 and MDCK cells (Supplemental Figure 1; Claypool *et al*., 2002). We find that CaM-Seph beads bound to the WT FcRn-tail GST-fusion protein, but not to GST alone (Figure 2A, lanes 3–6), and only in the presence of Ca^{2+} (Figure 2A, compare lane 5 with 6). Unconjugated Sepharose beads (Seph) did not bind to either GST or the WT FcRn-tail GST-fusion protein (Figure 2A, lanes 7 and 8). A second study shows that although the CaM-Seph beads bound to the WT FcRn-tail GST-fusion protein and the S303 mutant GST-fusion protein in the presence of Ca^{2+} (Figure 2B, lanes 1, 2, 7, and 8), the beads did not bind to the Del, R299A, or R300A mutant GST-fusion proteins (Figure 2B, lanes 3–6, 9, and 10). This is true for GST-fusion proteins solubilized in both NP-40- (Figure 2, A and B) and Triton X-100–based buffers (Supplemental Figure 2). To test whether calmodulin binding to the FcRn tail could be reversed upon removal of Ca^{2+}, we first incubated the GST-fusion proteins with CaM-Seph in the presence of Ca^{2+} to allow binding, and then we washed the beads in buffer containing Ca^{2+} or EGTA. As before, both the WT and S303A GST-fusion proteins bound CaM-Seph in the presence but not in the absence of Ca^{2+} (Figure 2C, lanes 4, 5, 8, and 9), and the Del mutant did not bind CaM-Seph (Figure 2C, lane 7). Chelating Ca^{2+} with EGTA completely reversed the binding of WT and S303A GST-fusion proteins to CaM-Seph (Figure 2C, lanes 6 and 10). Thus, calmodulin binding to the FcRn tail is direct, specific to the membrane-proximal region of the FcRn tail, dependent on the presence of Ca^{2+}, and reversible.

Disruption of the Calmodulin-binding Domain of FcRn in MDCK Cells Affects IgG Transcytosis

To test the function of the membrane-proximal domain of the FcRn cytoplasmic tail in intact cells, we prepared MDCK cells stably coexpressing human β_2m- and HA-tagged human FcRn heavy chain as described previously (Claypool *et al*., 2004). We expressed HA-tagged WT FcRn heavy chain and the R299A and R300A mutant forms of FcRn that cannot bind calmodulin in vitro, and an FcRn heavy chain lacking all but the first four amino-acid residues (RRMR) of the cytoplasmic tail (Tail-) (Figure 1B, right). As an additional control, we prepared MDCK cells expressing human β_2m and carrying an "empty" expression plasmid (vector control). The MDCK model faithfully reproduces all known aspects of FcRn-dependent bidirectional transcytosis of IgG across epithelial barriers (Claypool *et al*., 2002, 2004). Two independently derived MDCK cell clones for each construct were selected for further study based on the uniform expression of FcRn within polarized cell monolayers when analyzed by immunofluorescence microscopy (Figure 3A) and the expression of similar quantities of FcRn as assessed by immunoblot of whole cell lysates by using a mouse mAb to detect the HA-tag (Figure 3B). The distributions of the mutant FcRn heavy chains to a subapical supranuclear position in polarized MDCK monolayers were similar to WT FcRn (Figure 4A).

We first tested whether WT and mutant FcRn molecules expressed by the MDCK cell clones were folded correctly and retained the ability to bind IgG. Detergent extracts were prepared, adjusted to pH 6 or 8, and incubated with IgG-coupled Sepharose beads. In all clones tested, WT and mutant FcRn alike bound to IgG-Sepharose beads at pH 6 but not at pH 8 (Figure 3C). Thus, all the MDCK clones express FcRn molecules with a functional extracellular IgG-binding domain despite mutations present in their cytoplasmic tail domains.

To show that canine calmodulin can bind to the human FcRn cytoplasmic tail, detergent lysates of MDCK cells expressing WT FcRn were incubated with rabbit anti-calmodulin polyclonal antibodies, and immune complexes were precipitated with protein G-Sepharose and analyzed by immunoblot. Antibodies against calmodulin coimmunoprecipitated a small amount of FcRn from MDCK cell lysates in the absence of added Ca^{2+} and significantly more FcRn when Ca^{2+} was added to lysates (Figure 3D, compare lanes 2 and 3). Binding of canine calmodulin to FcRn was inhibited when EGTA was added to the detergent lysates (Figure 3D, lane 4). Similar results were obtained using calmodulin-Sepharose beads (data not shown). Thus, consistent with our in vitro results, canine calmodulin can bind human FcRn and this is Ca^{2+}-dependent.

Next, we measured the effect of the FcRn tail mutations on IgG transcytosis by using a recombinant humanized monoclonal IgG specific for the small hapten NIP as the FcRn ligand (Nip-IgG) (Claypool *et al*., 2004). In this assay, Nip-IgG is applied to apical or basolateral surfaces of MDCK monolayers, and transepithelial transport is measured in the contralateral reservoir by NIP-specific ELISA. Specificity for receptor-mediated transcellular transport is demonstrated by the addition of excess rabbit IgG that competes for binding to FcRn (Supplemental Figure 3). MDCK cells expressing FcRn mutants that cannot bind calmodulin (R299A and R300A), or that lack the cytoplasmic tail altogether (Tail-), transport Nip-IgG in both directions two- to fivefold less efficiently than MDCK cells expressing WT FcRn (Figure 3, E and F, and Supplemental Figure 3). Two independently derived clones expressing WT or each of the FcRn mutants gave the same results, showing that nonspecific clonal variations between cell lines cannot explain the defect in IgG transport (Figure 3, E and F). Remarkably, point mutations in the calmodulin-binding domain diminished Nip-IgG transport to nearly the same degree as deletion of the cytoplasmic tail altogether. MDCK cells that express human β_2m in the absence of FcRn heavy chain do not transport Nip-IgG in either direction, indicating that Nip-IgG transport is FcRn dependent (data not shown) (Claypool *et al*., 2002).

To test these results in another way, we examined the effect of pharmacologic inhibition of calmodulin using the small molecule W-7. Treatment of MDCK cell monolayers with W-7 (30 and 50 μM) reduced apical-to-basolateral Nip-IgG transcytosis by WT FcRn by $\geq$2-fold compared with untreated control cells (Figure 3G). The compound W-5 (50 μM), a less-potent analog of W-7, also reduced apical-to-basolateral Nip-IgG transcytosis (Supplemental Figure 4). To show specificity for calmodulin binding to FcRn, we applied W-7 to MDCK cells expressing FcRn mutants with inactivating mutations in the FcRn-calmodulin binding domain or lacking the cytoplasmic tail altogether. As before, W-7 inhibited Nip-IgG transport by WT FcRn, but had no effect on Nip-IgG transport by the R299A, R300A, and tail-

Figure 3 (cont). dently derived clones per construct were analyzed, and Nip-IgG transport was normalized to the mass of FcRn heavy chain detected in whole cell lysates (Figure 3B). The dashed line represents the average transport of Nip-IgG by tailless FcRn clones. (G and H) MDCK cell clones expressing WT or mutant FcRn were pretreated with buffer (control) or W-7 before addition of ligand. Data were normalized to transport by buffer-treated control cells (100%) (n is number of Transwells examined). Data represent one of two independent experiments demonstrating that W-7 has no effect on Nip-IgG transport by MDCK cells expressing FcRn mutants (R299A or R300A) and one of three independent experiments showing that W-7 has no effect on transport by MDCK cells expressing tailless FcRn. NS, nonstatistically different ($p > 0.05$).

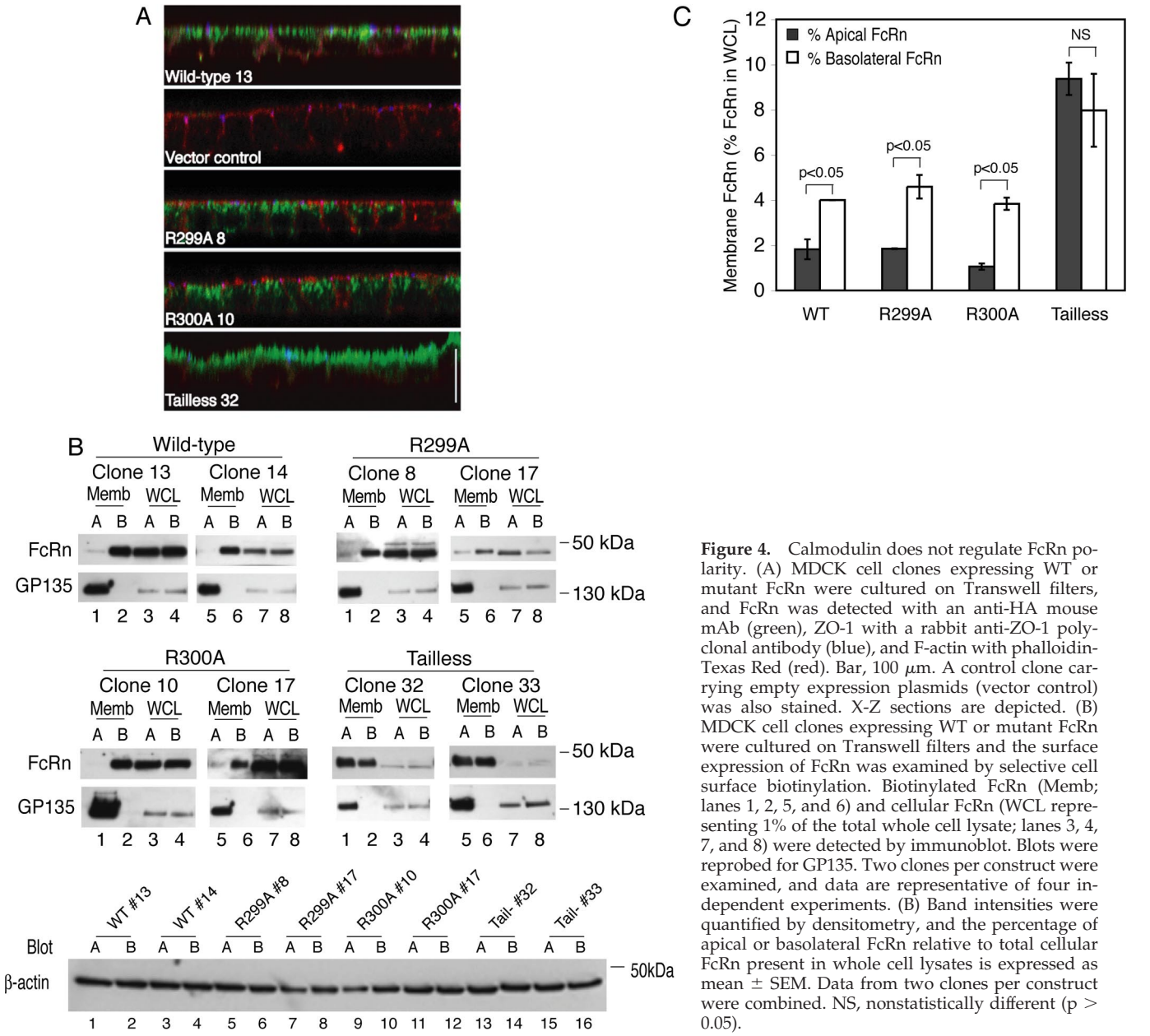

Figure 4. Calmodulin does not regulate FcRn polarity. (A) MDCK cell clones expressing WT or mutant FcRn were cultured on Transwell filters, and FcRn was detected with an anti-HA mouse mAb (green), ZO-1 with a rabbit anti-ZO-1 polyclonal antibody (blue), and F-actin with phalloidin-Texas Red (red). Bar, 100 μm. A control clone carrying empty expression plasmids (vector control) was also stained. X-Z sections are depicted. (B) MDCK cell clones expressing WT or mutant FcRn were cultured on Transwell filters and the surface expression of FcRn was examined by selective cell surface biotinylation. Biotinylated FcRn (Memb; lanes 1, 2, 5, and 6) and cellular FcRn (WCL representing 1% of the total whole cell lysate; lanes 3, 4, 7, and 8) were detected by immunoblot. Blots were reprobed for GP135. Two clones per construct were examined, and data are representative of four independent experiments. (B) Band intensities were quantified by densitometry, and the percentage of apical or basolateral FcRn relative to total cellular FcRn present in whole cell lysates is expressed as mean ± SEM. Data from two clones per construct were combined. NS, nonstatistically different ($p > 0.05$).

less FcRn mutants, consistent with an effect of W-7 on calmodulin binding to FcRn (Figure 3H). Thus, transport of IgG by FcRn in the transcytotic pathway is a function of the FcRn cytoplasmic tail, with strong dependence on the membrane-proximal domain that binds calmodulin.

Effect of Calmodulin on FcRn Cell Surface Polarity, Endocytosis, and Lysosomal Transport

We next tested for effects of mutations in the membrane-proximal region of the FcRn tail on the steady-state distribution of FcRn in polarized MDCK monolayers. The majority of WT FcRn (90–95%) resides in an intracellular compartment(s) below the apical plasma membrane, but the receptor occurs on the cell surface at steady state in small quantities. We have shown previously by selective cell surface biotinylation that the fraction of FcRn on the cell surface is strongly polarized to the basolateral membrane in MDCK cells. Targeting to the basolateral membrane must be a function of the FcRn cytoplasmic tail because the tailless FcRn mutant distributes nearly equally between both membrane domains (Claypool *et al.*, 2004). Here, we find that like WT FcRn, both the R299A and R300A FcRn mutants localize predominantly to an intracellular compartment(s) as assessed by confocal microscopy of MDCK monolayers stained for FcRn, F-actin, and ZO-1 (Figure 4A). Selective cell surface biotinylation of apical or basolateral membranes shows that most of the FcRn on the cell surface is localized to the basolateral membrane (Figure 4, B and C). Tailless FcRn is also localized to a compartment(s) inside the cell, but unlike WT FcRn and the R299A and R300A FcRn mutants, the fraction on the cell surface is evenly distributed between the apical and basolateral membranes, consistent with our previous results. To show that the intercellular junctions and cell surface polarity of the MDCK cell monolayers were

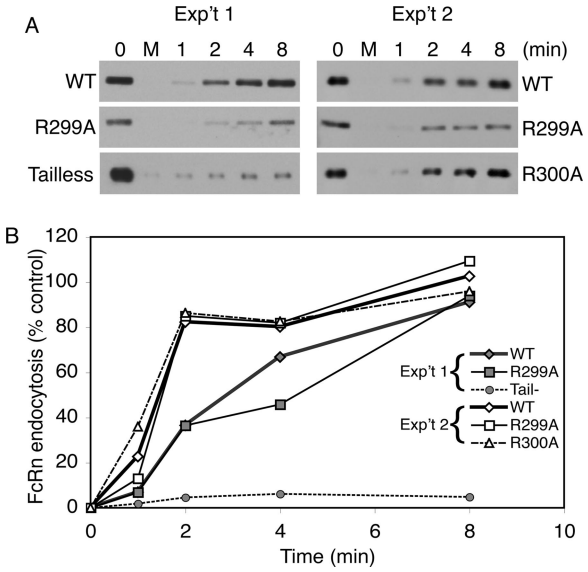

Figure 5. Calmodulin does not regulate FcRn endocytosis. (A) MDCK cell clones expressing WT or mutant FcRn cultured on Transwell filters were biotinylated on their basolateral aspect with sulfo-NHS-SS-biotin. Cells were cooled to 4°C and incubated at 37°C for 1, 2, 4, or 8 min and rapidly cooled to 4°C. Cell surface-associated biotin was removed with reduced glutathione at 4°C, and the cells were lysed in RIPA buffer. Two Transwells per clone were maintained at 4°C as a control (no reduction, time 0) and as a control for reduction (M, mock). Biotinylated FcRn was detected by immunoblot. (B) The mass of biotinylated FcRn was determined by densitometry. Two independent experiments are shown.

maintained during these experiments, we examined the cell surface polarity of the apical membrane protein GP135. GP135 remained restricted to the apical membrane domain as predicted. Cell lysates were analyzed for β-actin by immunoblot to demonstrate that equal quantities of cell lysates (assessed by protein content) were used in the avidin-agarose pull-downs (Figure 4B). Thus, the bulk of the R299A and R300A FcRn mutants distribute across polarized MDCK monolayers like WT FcRn, residing mostly within an intracellular compartment(s) at steady state. Unlike the tailless FcRn mutant, however, the point mutations in the membrane proximal calmodulin-binding domain of FcRn must leave intact the regions of the FcRn cytoplasmic tail that dictate polarized sorting to the basolateral membrane.

Endocytosis of WT and mutant FcRn was examined using a cleavable biotin-linker to label cell surface FcRn at 4°C. After warming the MDCK cell monolayers for the indicated times, biotin was cleaved from cell surface proteins and the mass of internalized FcRn labeled with biotin was measured in total cell lysates by affinity precipitation with streptavidin beads, SDS-PAGE, and immunoblot for FcRn with the anti-HA antibody (Figure 5). These studies show that the R299A and R300A calmodulin-binding mutants of FcRn entered MDCK cells as efficiently as WT FcRn. Endocytosis of the tail-minus FcRn mutant, however, was strongly inhibited, consistent with loss of the dileucine and tryptophan endocytosis motifs contained within the tail-domain.

We next tested for effects of the calmodulin-binding domain on sorting into the late endosome/lysosome pathway by measuring the half-life of FcRn. In initial studies, we measured the half-life of posttranslationally modified FcRn already located at the cell surface. In these studies, the basolateral membranes of MDCK cells expressing WT and mutant FcRn were biotinylated at 4°C, washed, and cells were then returned to 37°C for 0, 6, 12, or 24 h. At each interval, biotin-labeled FcRn in cell lysates was captured on avidin-agarose beads and detected by immunoblot (Figure 6A; see Supplemental Figure 5 for more detailed time course). Compared with WT FcRn ($t_{1/2} \sim 12$ h), the cell surface fraction of R299A ($t_{1/2} \sim 9$ h), R300A ($t_{1/2} \sim 5$ h), and tailless ($t_{1/2} \sim 10$ h) FcRn mutants were always less (Figure 6B), suggesting more rapid degradation.

We also tested this idea by metabolic labeling of MDCK cells expressing WT and mutant FcRn with [^{35}S]methionine/cysteine followed by chase in "cold" medium for up to 48 h. At the indicated times, FcRn was immunoprecipitated from total cell lysates, and the mass of ^{35}S-labeled FcRn was measured by SDS-PAGE and autoradiography (Figure 6C). These data were quantified and normalized to the mass of ^{35}S-FcRn present at the initial 6-h interval so as to control for degradation of misfolded or unassembled proteins that never enter the secretory pathway (Figure 6D). As observed in the studies described above, the R299A and R300A FcRn mutants, and tailless FcRn are degraded more rapidly compared with WT FcRn. Thus, FcRn mutants that cannot bind calmodulin seem to sort away from the lysosomal pathway less efficiently than WT FcRn.

To confirm specificity for calmodulin-binding to FcRn in lysosomal transport by another method, we again used the small molecule W-7 to inhibit calmodulin function (Figure 6E). Here, we find that treatment of MDCK monolayers expressing WT FcRn with W-7 caused a marked (~50%) reduction in the mass of cell surface biotin-labeled-FcRn after 3-h chase, consistent with a dependency for FcRn binding to calmodulin in this pathway. However, unlike our results in the transcytosis studies, treatment with W-7 also affected degradation of the tailless mutant FcRn that cannot bind calmodulin. This result suggests a generalized or nonspecific effect of longer treatments with W-7 on lysosomal transport (or function) in MDCK cells, and precludes testing the hypothesis by this approach.

Ca^{2+}-dependent Binding of Calmodulin to FcRn and Regulation of IgG Transcytosis in Human Intestinal T84 Cells

To see whether our results might be applied as a general rule, we tested for interaction between calmodulin and FcRn in the human intestinal cell line T84. T84 cells form polarized epithelial barriers, express endogenous FcRn, and transport IgG across the monolayer by FcRn-dependent transcytosis (Dickinson *et al*., 1999). To test for FcRn binding, an anti-calmodulin mouse mAb (CaM mAb) was used to immunoprecipitate calmodulin from detergent lysates of T84 cells in the presence or absence of Ca^{2+}. For these biochemical studies, we used retrovirus transfected T84 cell clones overexpressing the human FcRn α chain (T84-FcRn) (Figure 7A). The immunoprecipitates from total cell lysates were analyzed for FcRn by immunoblot by using a rabbit antibody raised against the WT GST-FcRn tail fusion protein, and which specifically binds to the tail domain of FcRn as assessed in both T84 and MDCK cells expressing the receptor (Supplemental Figure 1) (Claypool *et al*., 2004). The CaM mAb immunoprecipitated FcRn in the presence but not in the absence of Ca^{2+} (Figure 7B, compare lanes 1 and 2 with lane 3), suggesting a physical interaction between the two molecules. To test this result in another way, we used CaM-Seph beads. As in the coimmunoprecipitations studies, CaM-Seph beads bound FcRn from T84-FcRn lysates in the presence but in not the absence of Ca^{2+} (Figure 7C, compare lanes 4 and 6). Excess soluble calmodulin in the presence of

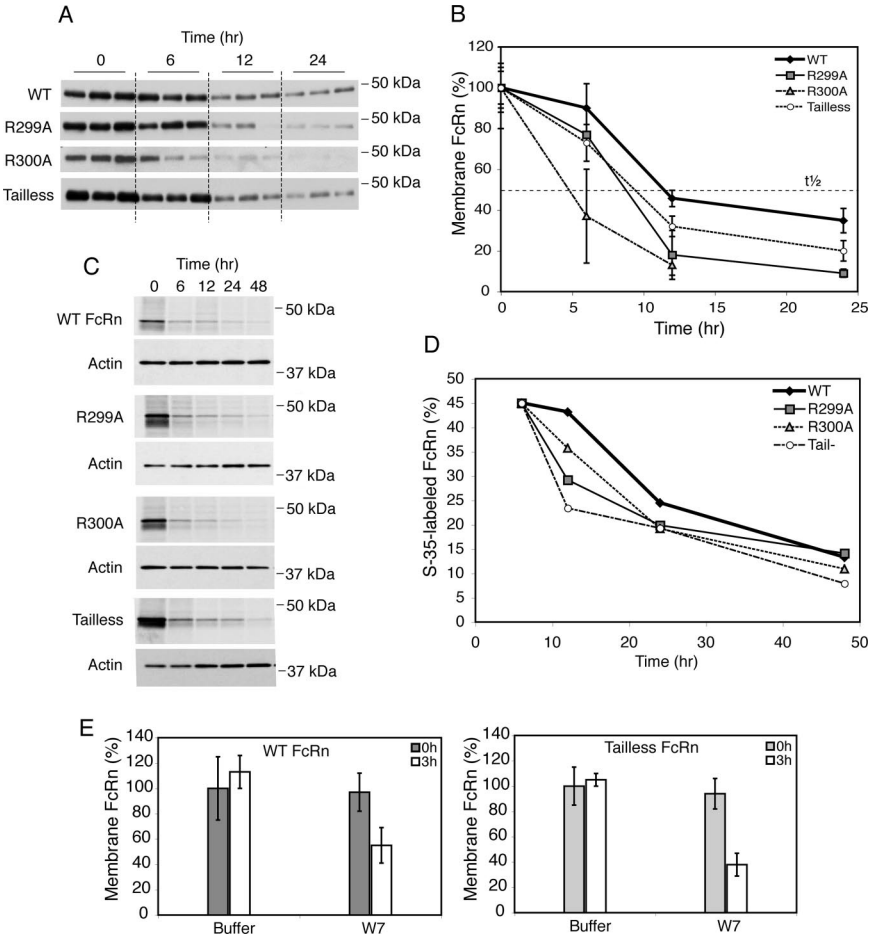

Figure 6. Calmodulin regulates FcRn half-life. The basolateral membrane of MDCK cell clones cultured on Transwell filters was biotinylated, and the cells were incubated for 0–24 h at 37°C. At intervals, biotinylated FcRn was detected by immunblot (A) and quantified by densitometry (B). The mass of biotinylated FcRn is expressed as a percentage of the starting mass of FcRn at time 0 h (100%). $t_{1/2}$ indicates the time at which 50% of the initial FcRn-biotin signal is detected. Data are representative of three independent experiments. (C) MDCK cells were cultured on Transwell filters and metabolically labeled with [^{35}S]methionine/cysteine and chased in cold medium for 48 h. At intervals, FcRn was immunoprecipitated from lysates and radiolabeled FcRn was detected by autoradiography (top). β-Actin was detected by immunoblot to demonstrate equal loading (bottom). (D) Bands were quantified by densitometry, and the percentage of radiolabeled FcRn at each time point is expressed relative to the quantity of FcRn at the 6-h time point (45 $\pm$ 4.3%). Data are representative of three independent experiments. (E) MDCK cells expressing WT or tailless FcRn cultured on Transwell inserts were pretreated with buffer or 50 μM W-7 for 20 min at 37°C, cooled to 4°C, and biotinylated on their basolateral aspect. Cells were either lysed directly (0 h) or incubated in medium alone or medium containing 50 μM W-7 for 3 h at 37°C. Biotinylated-FcRn present in the cell was assessed by avidin-agarose precipitation and immunoblot. Three Transwells per condition were examined.

Ca^{2+} competed for FcRn binding and inhibited FcRn binding to the CaM-Seph beads, as predicted for a specific binding reaction (Figure 7C, compare lanes 4 and 8). Thus, in the presence of Ca^{2+}, endogenous calmodulin specifically binds FcRn expressed in T84 cells, consistent with a regulatory role for calmodulin in FcRn function.

To test whether calmodulin affects FcRn function in T84 cells expressing the endogenous receptor, we used the calmodulin antagonist W-7 to inhibit calmodulin action. In this experiment, biotin-labeled human IgG (IgG-biotin) was applied to the basolateral cell surface of T84 cells and detected on the opposite surface by SDS-PAGE and avidin-HRP im-

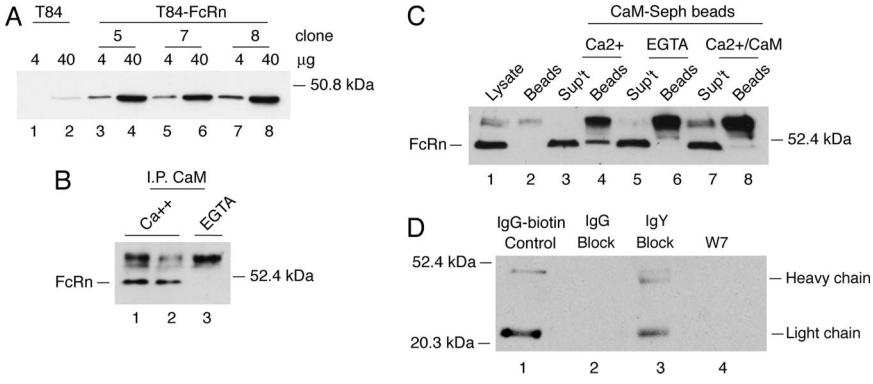

Figure 7. Calmodulin binds to FcRn expressed in human T84 cells and regulates FcRn-dependent IgG transcytosis. (A) T84 cells (lanes 1 and 2) and T84 cells overexpressing human FcRn (T84-FcRn clones 5, 7, and 8; lanes 3–8) were lysed and examined for FcRn expression by immunoblot. (B) T84-FcRn cell lysates containing calcium (lanes 1 and 2) or EGTA (lane 3) were incubated with protein G-Sepharose beads covalently coupled to an anti-calmodulin mAb. FcRn bound to the beads was detected by immunoblot. Nonspecific bands associated with the protein G-Sepharose beads cross-react with the rabbit antiserum and are shown in each lane above the 52.4-kDa molecular weight marker. (C) T84-FcRn cell lysates containing calcium (lanes 3 and 4), EGTA (lanes 5 and 6), or excess bovine brain calmodulin (lanes 7 and 8) were incubated with calmodulin-Sepharose beads. FcRn bound to the beads (lanes 4, 6, and 8) or retained in the nonbinding fraction (sup't) were detected by immunoblot. FcRn present in whole cell lysates is shown as a control in lane 1. A high-molecular-weight cross-reactive band released from calmodulin-Sepharose beads is shown in lane 2 and in each sample containing beads (lanes 4, 6, and 8). (D) Basolateral-to-apical transcytosis of biotinylated human IgG (IgG-biotin) was examined in T84 cells pretreated with excess underivatized human IgG (lane 2), chicken IgY (lane 3), or W-7 (lane 4) before addition of ligand. Transport of IgG-biotin into the apical buffer was assessed by avidin-HRP immunoblot. Ligand is shown in lane 1 as a control. Results are representative of four independent experiments.

munoblot (Figure 7D). To demonstrate specificity for FcRn-dependent transport, the IgG-biotin was applied in the presence of 500-fold molar excess unlabeled human IgG or chicken IgY. Chicken IgY does not bind FcRn, but it is structurally similar to human IgG. These studies show that FcRn transports IgG across T84 cell monolayers in the presence of excess IgY but not in the presence of excess human IgG (Figure 7D, compare lanes 2 and 3). The complete competition by human IgG for IgG-biotin transport across T84 cells demonstrates that the monolayers are impermeant to IgG flux by passive diffusion across intercellular tight junctions and that transport is specific to FcRn. The calmodulin antagonist W-7 at 30 μM inhibits IgG-biotin transcytosis in T84 cells (Figure 7D, compare lanes 3 and 4), consistent with a role for calmodulin in FcRn-dependent IgG transcytosis.

DISCUSSION

The results of this study identify a calmodulin-binding motif in the FcRn cytoplasmic tail that regulates bidirectional IgG transcytosis and FcRn half-life by affecting sorting between the transcytotic and degradative pathways. Calmodulin binding to this region of the FcRn tail in vitro is reversible and Ca^{2+} dependent, consistent with a regulatory function for the calmodulin-binding motif in vivo. The motif seems to act by binding calmodulin in intact cells, because calmodulin and FcRn coimmunoprecipitate from cell lysates in the presence of Ca^{2+}, and because the calmodulin antagonist W-7 reproduces the functional defect in FcRn-dependent IgG transcytosis caused by inactivating mutations in the calmodulin-binding domain. Because FcRn is already known to transport immune complexes in the intestine with functional consequences (Yoshida *et al*., 2004, 2006), the regulated sorting between transcytotic and degradative pathways likely affects antigen processing at mucosal surfaces in fundamental ways.

In both the transcytosis and half-life assays for FcRn function, we find that single inactivating amino acid substitutions within the FcRn calmodulin-binding domain cause the same or similar degrees of inhibition as deletion of the entire FcRn cytoplasmic tail. Thus, with respect to transcytosis, the calmodulin-binding domain has a dominant effect over the other sorting motifs contained within the cytoplasmic tail. This is not true, however, for the sorting motifs that dictate the polarity of cell surface expression at steady state. Here, the basolateral predominance of cell surface expression for the calmodulin-binding mutants is maintained like WT FcRn. Endocytosis motifs are also not affected. We also note that mutant FcRn R299A, R300A, and tailless FcRn remain capable of transporting IgG across the epithelial monolayer, although much less efficiently than the WT receptor. Thus, the FcRn cytoplasmic tail is ultimately dispensable for transcytosis, at least in cell culture models. These results are consistent with a previous study on rat FcRn expressed in rat inner medullary collecting duct cells (McCarthy *et al*., 2001). In this cell type, tailless rat FcRn was able to mediate basolateral-to-apical transcytosis of IgG, although transcytosis in the opposite direction was inhibited. In our study, tailless human FcRn displays a strong defect in transcytosis of IgG in both directions across MDCK cells.

The FcRn cytoplasmic tail and the calmodulin-binding domain seem to confer upon FcRn the characteristic of a prolonged half-life. Because we have studied cell surface FcRn fully processed through the biosynthetic pathway, the effect on half-life most likely has to do with sorting motifs in the FcRn cytoplasmic tail that direct FcRn and its cargo away from the late endosome/lysosome after endocytosis. Mutations in the calmodulin-binding domain, however, do not affect the steady-state distribution of FcRn in polarized epithelial cells, whereas with WT FcRn, the bulk of mutant receptors (R299A, R300A, and tailless FcRn) are found in intracellular compartments, possibly representing the recycling or common endosome (Ober *et al*., 2004; Ward *et al*., 2005). Thus, we propose that the site of action for calmodulin binding to FcRn occurs in this intracellular compartment where the degradative and transcytotic pathways are related by this sorting step.

Calmodulin has diverse effects on membrane dynamics and seems to affect transferrin receptor (TfnR) recycling (Hunt and Marshall-Carlson, 1986; Grasso *et al*., 1990; Sainte-Marie *et al*., 1997; Huber *et al*., 2000) and trafficking of the polymeric immunoglobulin receptor (pIgR) (Apodaca *et al*., 1994; Hunziker, 1994) in ways similar to that found for FcRn. Calmodulin binds directly to the membrane-proximal 17-amino-acid segment of the pIgR cytoplasmic tail, and it is possible this affects receptor trafficking in the transcytotic pathway, as proposed here for FcRn; but this has not yet been tested at the molecular level (Chapin *et al*., 1996). The way calmodulin affects TfnR trafficking is indirect, by acting via a Ca^{2+}-independent reaction on the unconventional myosin Myr4 (Huber *et al*., 2000).

How might calmodulin work to affect structure and function of FcRn in polarized epithelial cells? Recent studies show that amphipathic α-helices similar to the calmodulin-binding domain in FcRn, and to motifs found in Epsin and Sar1, can partially integrate into cell membranes so as to induce or sense membrane curvature and thus affect membrane dynamics (Ford *et al*., 2002; Lee *et al*., 2005; McMahon and Gallop, 2005). This is also true of the huntingtin protein that contains a motif with a predicted amphipathic α-helix capable of inserting into lipid bilayers to anchor the protein to specific membrane domains (Kegel *et al*., 2005). Amphipathic α-helices can exhibit specific affinities for different membrane phospholipids, which may provide additional specificity to domain function (Nakanishi *et al*., 2004). Here, we identify a putative amphipathic α-helix in FcRn located immediately adjacent to the membrane, where it could, as in these other proteins, reversibly integrate into the membrane so as to affect membrane dynamics and receptor sorting. Calmodulin binding to this domain would be predicted to reversibly mask the α-helix and allow for this function to be physiologically regulated.

Another way calmodulin binding to the FcRn tail might affect FcRn function could be by masking sites for cycles of phosphorylation and dephosphorylation. In FcRn, a serine residue lies within the basic region of the putative amphipathic α-helix where calmodulin binds, and other potential phosphorylation sites for calmodulin-dependent kinase II, casein kinase I, and protein kinases A or C are located nearby. Among other ways phosphorylation can affect membrane transport, phosphorylation and dephosphorylation cycles on residues located in or near the basic region of such amphipathic α-helices would alter the electrical potential of these protein surfaces so as to affect membrane association and domain function. The myristoylated alanine-rich C kinase substrate protein (MARCKS) is a good example of this mechanism where the basic region of the amphipathic domain in MARCKS binds calmodulin in the presence of Ca^{2+} (Graff *et al*., 1989; McIlroy *et al*., 1991; Taniguchi and Manenti, 1993), and this is regulated by phosphorylation (Swierczynski and Blackshear, 1996).

Thus, based on our results, we propose that calmodulin binding to the membrane-proximal region of the FcRn cytoplasmic tail provides a physiologically reversible "molecular

switch" for regulating the trafficking of FcRn and its ligand IgG away from the degradative lysosomal pathway and into the transcytotic pathway of polarized epithelial cells.

ACKNOWLEDGMENTS

This work was supported by National Institutes of Health (NIH) Career Development Award DK-059945 (to B.L.D.), and NIH grants DK-48106 (to W.I.L.), DK-44319 and DK-51362 (R.S.B.), and DK53056 (to R.S.B. and W.I.L.). B.L.D. is a recipient of the Harvard Digestive Diseases Center Pilot/Feasibility award (DK-34854), and a recipient of a Crohn's and Colitis Foundation of America Senior Scientist Award (1114).

REFERENCES

Apodaca, G., Enrich, C., and Mostov, K. E. (1994). The calmodulin antagonist, W-13, alters transcytosis, recycling, and the morphology of the endocytic pathway in Madin-Darby canine kidney cells. J. Biol. Chem. *269*, 19005–19013.

Bitonti, A. J. *et al*. (2004). Pulmonary delivery of an erythropoietin Fc fusion protein in non-human primates through an immunoglobulin transport pathway. Proc. Natl. Acad. Sci. USA *101*, 9763–9768.

Borvak, J., Richardson, J., Medesan, C., Antohe, F., Radu, C., Simionescu, M., Ghetie, V., and Ward, E. S. (1998). Functional expression of the MHC class I-related receptor, FcRn, in endothelial cells of mice. Int. Immunol. *10*, 1289–1298.

Burmeister, W. P., Gastinel, L. N., Simister, N. E., Blum, M. L., and Bjorkman, P. J. (1994). Crystal structure at 2.2 A resolution of the MHC-related neonatal Fc receptor. Nature *372*, 336–343.

Chapin, S. J., Enrich, C., Aroeti, B., Havel, R. J., and Mostov, K. E. (1996). Calmodulin binds to the basolateral targeting signal of the polymeric immunoglobulin receptor. J. Biol. Chem. *271*, 1336–1342.

Chin, D., and Means, A. R. (2000). Calmodulin: a prototypical calcium sensor. Trends Cell Biol. *10*, 322–328.

Claypool, S. M., Dickinson, B. L., Wagner, J. S., Johansen, F.-E., Venu, N., Borawski, J. A., Lencer, W. I., and Blumberg, R. S. (2004). Bidirectional transepithelial IgG transport by a strongly polarized basolateral membrane Fc{gamma}-receptor. Mol. Biol. Cell *15*, 1746–1759.

Claypool, S. M., Dickinson, B. L., Yoshida, M., Lencer, W. I., and Blumberg, R. S. (2002). Functional reconstitution of human FcRn in Madin-Darby canine kidney cells requires co-expressed human beta 2-microglobulin. J. Biol. Chem. *277*, 28038–28050.

Colgan, S. P., Hershberg, R. M., Furuta, G. T., and Blumberg, R. S. (1999). Ligation of intestinal epithelial CD1d induces bioactive IL-10, critical role of the cytoplasmic tail in autocrine signaling. Proc. Natl. Acad. Sci. USA *96*, 13938–13943.

Dickinson, B. L., Badizadegan, K., Wu, Z., Ahouse, J. C., Zhu, X., Simister, N. E., Blumberg, R. S., and Lencer, W. I. (1999). Bidirectional FcRn-dependent IgG transport in a polarized human intestinal epithelial cell line. J. Clin. Investig. *104*, 903–911.

Ford, M. G., Mills, I. G., Peter, B. J., Vallis, Y., Praefcke, G. J., Evans, P. R., and McMahon, H. T. (2002). Curvature of clathrin-coated pits driven by epsin. Nature *419*, 361–366.

Graff, J. M., Young, T. N., Johnson, J. D., and Blackshear, P. J. (1989). Phosphorylation-regulated calmodulin binding to a prominent cellular substrate for protein kinase C. J. Biol. Chem. *264*, 21818–21823.

Grasso, J. A., Bruno, M., Yates, A. A., Wei, L. T., and Epstein, P. M. (1990). Calmodulin dependence of transferrin receptor recycling in rat reticulocytes. Biochem. J. *266*, 261–272.

Hershberg, R. M., Framson, P. E., Cho, D. H., Lee, L. Y., Kovats, S., Beitz, J., Blum, J. S., and Nepom, G. T. (1997). Intestinal epithelial cells use two distinct pathways for HLA class II antigen processing. J. Clin. Invest. *100*, 204–215.

Huber, A. H., Kelley, R. F., Gastinel, L. N., and Bjorkman, P. J. (1993). Crystallization and stoichiometry of binding of a complex between a rat intestinal Fc receptor and Fc. J. Mol. Biol. *230*, 1077–1083.

Huber, L. A., Fialka, I., Paiha, K., Hunziker, W., Sacks, D. B., Bahler, M., Way, M., Gagescu, R., and Gruenberg, J. (2000). Both calmodulin and the unconventional myosin Myr4 regulate membrane trafficking along the recycling pathway of MDCK cells. Traffic *1*, 494–503.

Hunt, R. C., and Marshall-Carlson, L. (1986). Internalization and recycling of transferrin and its receptor. Effect of trifluoperazine on recycling in human erythroleukemic cells. J. Biol. Chem. *261*, 3681–3686.

Hunziker, W. (1994). The calmodulin antagonist W-7 affects transcytosis, lysosomal transport, and recycling but not endocytosis. J. Biol. Chem. *269*, 29003–29009.

Kegel, K. B. *et al*. (2005). Huntingtin Associates with Acidic Phospholipids at the Plasma Membrane. J. Biol. Chem. *280*, 36464–36473.

Lee, M. C., Orci, L., Hamamoto, S., Futai, E., Ravazzola, M., and Schekman, R. (2005). Sar1p N-terminal helix initiates membrane curvature and completes the fission of a COPII vesicle. Cell *122*, 605–617.

McCarthy, K. M., Lam, M., Subramanian, L., Shakya, R., Wu, Z., Newton, E. E., and Simister, N. E. (2001). Effects of mutations in potential phosphorylation sites on transcytosis of FcRn. J. Cell Sci. *114*, 1591–1598.

McIlroy, B. K., Walters, J. D., Blackshear, P. J., and Johnson, J. D. (1991). Phosphorylation-dependent binding of a synthetic MARCKS peptide to calmodulin. J. Biol. Chem. *266*, 4959–4964.

McMahon, H. T., and Gallop, J. L. (2005). Membrane curvature and mechanisms of dynamic cell membrane remodelling. Nature *438*, 590–596.

Nakanishi, H., de los Santos, P., and Neiman, A. M. (2004). Positive and negative regulation of a SNARE protein by control of intracellular localization. Mol. Biol. Cell *15*, 1802–1815.

Ober, R. J., Martinez, C., Vaccaro, C., Zhou, J., and Ward, E. S. (2004). Visualizing the site and dynamics of IgG salvage by the MHC class I-related receptor, FcRn. J. Immunol. *172*, 2021–2029.

Raghavan, M., Gastinel, L. N., and Bjorkman, P. J. (1993). The class I major histocompatibility complex related Fc receptor shows pH-dependent stability differences correlating with immunoglobulin binding and release. Biochemistry *32*, 8654–8660.

Rhoads, A., and Friedberg, F. (1997). Sequence motifs for calmodulin recognition. FASEB J. *11*, 331–340.

Rodewald, R. (1976). pH-dependent binding of immunoglobulins to intestinal cells of the neonatal rat. J. Cell Biol. *71*, 666–669.

Sainte-Marie, J., Lafont, V., Pecheur, E. I., Favero, J., Philippot, J. R., and Bienvenue, A. (1997). Transferrin receptor functions as a signal-transduction molecule for its own recycling via increases in the internal Ca2+ concentration. Eur. J. Biochem. *250*, 689–697.

Spiekermann, G. M., Finn, P. W., Ward, E. S., Dumont, J., Dickinson, B. L., Blumberg, R. S., and Lencer, W. I. (2002). Receptor-mediated immunoglobulin G transport across mucosal barriers in adult life: functional expression of FcRn in the mammalian lung. J. Exp. Med. *196*, 303–310.

Stefaner, I., Praetor, A., and Hunziker, W. (1999). Nonvectorial surface transport, endocytosis via a Di-leucine-based motif, and bidirectional transcytosis of chimera encoding the cytosolic tail of rat FcRn expressed in Madin-Darby canine kidney cells. J. Biol. Chem. *274*, 8998–9005.

Swierczynski, S. L., and Blackshear, P. J. (1996). Myristoylation-dependent and electrostatic interactions exert independent effects on the membrane association of the myristoylated alanine-rich protein kinase C substrate protein in intact cells. J. Biol. Chem. *271*, 23424–23430.

Taniguchi, H., and Manenti, S. (1993). Interaction of myristoylated alanine-rich protein kinase C substrate (MARCKS) with membrane phospholipids. J. Biol. Chem. *268*, 9960–9963.

Ward, E. S., Martinez, C., Vaccaro, C., Zhou, J., Tang, Q., and Ober, R. J. (2005). From sorting endosomes to exocytosis: association of Rab4 and Rab11 GTPases with the Fc receptor, FcRn, during recycling. Mol. Biol. Cell *16*, 2028–2038.

Ward, E. S., Zhou, J., Ghetie, V., and Ober, R. J. (2003). Evidence to support the cellular mechanism involved in serum IgG homeostasis in humans. Int. Immunol. *15*, 187–195.

Wu, Z., and Simister, N. E. (2001). Tryptophan- and dileucine-based endocytosis signals in the neonatal Fc receptor. J. Biol. Chem. *276*, 5240–5247.

Yoshida, M., Claypool, S. M., Wagner, J. S., Mizoguchi, E., Mizoguchi, A., Roopenian, D. C., Lencer, W. I., and Blumberg, R. S. (2004). Human neonatal Fc receptor mediates transport of IgG into luminal secretions for delivery of antigens to mucosal dendritic cells. Immunity *20*, 769–783.

Yoshida, M. *et al*. (2006). Neonatal Fc receptor for IgG regulates mucosal immune responses to luminal bacteria. J. Clin. Invest. *116*, 2142–2151.

Zhao, Y., Kacskovics, I., Hao, Z., and Hammarstrom, L. (2003). Presence of the di-leucine motif in the cytoplasmic tail of the pig FcRn α chain. Vet. Immunol. Immunopathol. *96*, 229–233.